Received 21 February 2023; revised 29 March 2023; accepted 22 April 2023. Date of publication 26 April 2023; date of current version 4 May 2023.
The review of this article was arranged by Editor A. Nathan.

Digital Object Identifier 10.1109/JEDS.2023.3270583

Quantitative Measurement of Interface State Density in Donor-Acceptor Polymer Transistors

BIAOBIAO DING[1], YICHEN ZHU[2], RUN LI[3], GUANGAN YANG[1], JIE WU[1], LI ZHU[1], XIANG WAN[1], ZHIHAO YU[1], CHEE LEONG TAN[1], YONG XU[1], AND HUABIN SUN[1]

1 College of Integrated Circuit Science and Engineering, Nanjing University of Posts and Telecommunications, Nanjing 210023, Jiangsu, China
2 College of Electronics and Optical Engineering and the College of Flexible Electronics (Future Technology), Nanjing University of Posts and Telecommunications, Nanjing 210023, Jiangsu, China
3 Guangdong Greater Bay Area Institute of Integrated Circuit and System, Guangzhou 510535, Guangdong, China

CORRESPONDING AUTHORS: H. SUN, C. L. TAN, AND G. YANG (e-mail: hbsun@njupt.edu.cn; cheelong@njupt.edu.cn; yga_njupt@163.com)

This work was supported in part by the National Natural Science Foundation of China under Grant 52105369, Grant 61974070, and Grant M0604; in part by the Natural Science Foundation of the Jiangsu Higher Education Institutions of China under Grant 20KJB460008; in part by the Natural Science Foundation of Jiangsu Province, China, under Grant BK20190725, Grant BK20180759, and Grant BK20200746; in part by NUPTSF under Grant NY220066, Grant NY219139, Grant NY218149, and Grant NY220077; in part by the High-Level Innovation Research Institute from Guangdong Province Research and Development in Key Fields through the Guangdong Greater Bay Area Institute of Integrated Circuit and System under Grant 2021B0101280002; and in part by the Guangzhou City Research and Development Program in Key Field under Grant 20210302001.

This article has supplementary downloadable material available at https://doi.org/10.1109/JEDS.2023.3270583, provided by the authors.

ABSTRACT Donor-Acceptor (D-A) polymer field-effect transistors (pFETs) are at the cutting edge of organic electronics. However, some fundamental cognition of interface states remains unquantified, particularly at different dynamic scales. In this study, the interface states of D-A polymer transistors are quantified using the dynamic pumping method. The experimental results indicate that the interface state density of the transistor is insensitive to the measurement pulse condition and stays within the range of $10^{12} \sim 10^{13}$ cm^{-2}. The experiments described in this paper provide a quantitative analysis of interface states. This analysis can serve as effective guidance for optimizing future devices.

INDEX TERMS Dynamic pumping, interface state density, organic transistor, polymer.

I. INTRODUCTION

The development of stretchable electronics has significantly broadened the range of applications for electronic devices, including medical devices, medical testing, and brain-machine interfaces [1], [2], [3], [4]. In the healthcare industry, stretchable devices can be used to develop non-invasive monitoring and treatment applications for conditions such as diabetes and cardiovascular disease [5], [6]. Frequently, these devices are fabricated with novel materials or device structures that possess the exceptional ability to stretch and bend without breaking.

Polymer transistors have the potential to play a crucial role in the development of stretchable devices due to their simple fabrication using low-cost and scalable technologies. Donor-Acceptor (D-A) polymers can now be used to create stretchable transistors with enhanced performance [7], [8], [9]. In-depth knowledge of device physics is necessary for the optimization of the performance of polymer transistor devices. The study of interfacial conditions, for instance, can aid in the exhaustive optimization of carrier transport.

The distribution of interfacial states in D-A polymer transistors is a key factor affecting the dynamic performance of these devices [10], [11], [12], [13]. Most previous studies on the interfacial states of D-A polymer transistors have relied on static or quasi-static techniques [14], [15], [16] However, the recovery of the device response due to stress occurs within the measurement time [17], [18]. Since logic devices often operate over a wide frequency range, device interface information obtained during fast operation is critical for evaluating transistors [19]. Dynamic techniques, such as charge pumping, can be used to examine the interface state of polymer transistors over a range of time scales [20], [21], [22], [23]. Charge pumping allows for a more accurate description of the polymer transistor's interfacial state. The charge pumping can more accurately characterize the carrier capture and release in the channel by measuring the

interfacial state over a shorter time range [24], [25], [26]. This allows for a more accurate evaluation of the polymer transistor during dynamic operation. The charge pumping approach provides useful insight into the dynamic behavior of polymer transistors by examining the interface states in multiple time domains [20], [21]. In contrast to conventional silicon devices, since carrier generation in polymer semiconductors is dependent on the injection of active regions, we borrowed the charge pumping principle and employed a dynamic pumping technique to characterize the interfacial states of polymer transistors.

Using a dynamic pumping technique, the interfacial state of a polymer transistor is quantified in this work. We measure the source-drain current while a series of gate pulses are applied. The state density distribution on the highest occupied molecular orbital (HOMO) energy level was determined by analyzing the change in pump current at various gate pressures.The interface trap density was evaluated in the fall time range of 20 μs to 1 ms. Our findings indicate that the interface trap density of states of the transistor does not vary significantly with frequency of operation, remaining between 10^{12}cm^{-2} and 10^{13}cm^{-2}.

Fig. 1(a) depicts the top-gate bottom-contact structure of a diketopyrrolopyrrole-thieno[3,2-b]thiophene (DPPT-TT) polymer p-type transistor. Fig. 1(b) show the optical images. The semiconducting layer of this transistor is composed of DPPT-TT, while its gate dielectric is composed of polymethyl methacrylate (PMMA). On a glass substrate, 50 nm/5 nm thick Au/Ni is thermally evaporated under a vacuum to create the source and drain electrodes. The DPPT-TT solution (5 mg mL^{-1} in 1,2-Dichlorobenzene) is then spin-coated for 60 seconds at 2000 rpm, followed by an hour of annealing at 150 °C. The solution of PMMA (100 mg mL^{-1} in n-Butyl acetate) is then spin-coated at 2,000 rpm for 60 seconds and annealed at 80 °C for 4 hours. The gate on the PMMA layer is then generated by thermally evaporating 100 nm of aluminum under a vacuum. The device being used has a channel length of 300 μm and a width of 1200 μm. The molecular weight of PMMA is 120,000 Mw. The spin-coating and annealing processes are conducted in a nitrogen-filled glove box.

I-V measurements were conducted utilizing a Keysight B1500A meter. The linear region transfer characteristics of the polymer transistor are demonstrated in Fig. 1(c). The threshold voltage, subthreshold swing, and field mobility are, respectively, −2.94 V, 3.75 V dec^{-1}, and 0.12 cm^{2}V^{-1}s^{-1}. Fig. 1(d) displays the output curve of the transistor. Indicating the metal-polymer contact type to be nearly ohmic and the leakage to be negligible, all of the output curves intersect zero and display a high degree of linearity in the expanded image, ultimately not hindering the device's performance. All electrical measurements were performed at room temperature and in an atmosphere.

Fig. 2(a) represents the time domain dynamic pumping measurement scheme. The SPGU module of the B1500A generates the gate pulse signal, while the OPA 657 amplifies

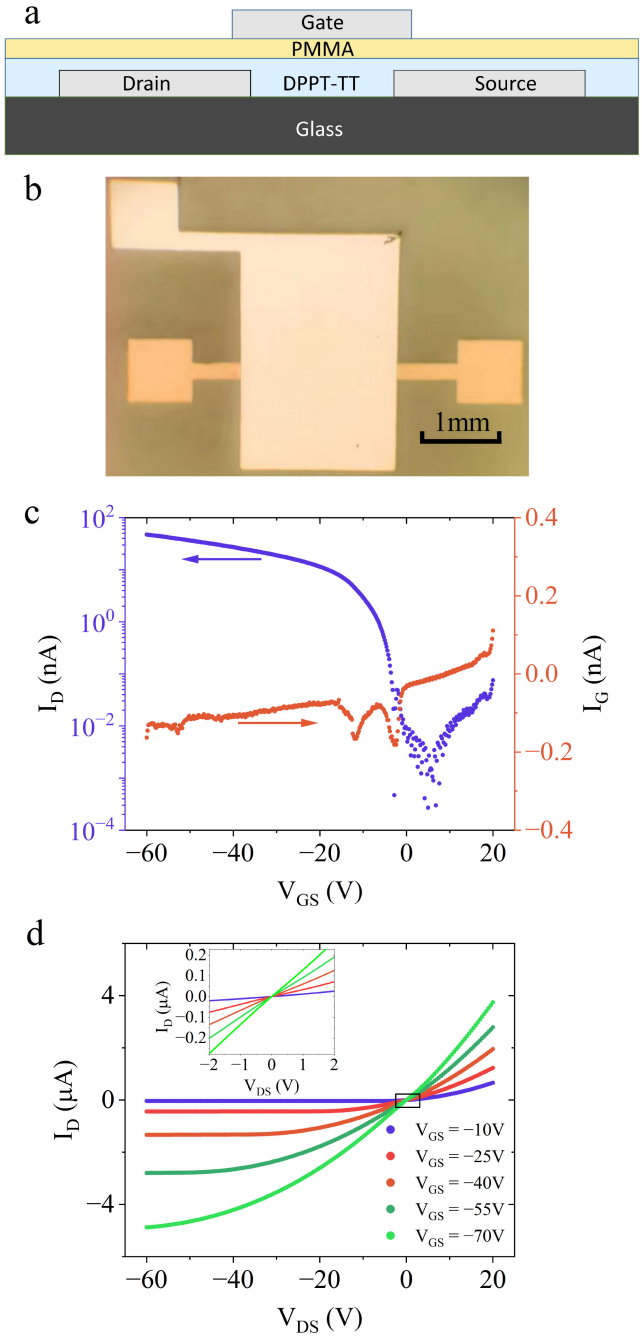

FIGURE 1. (a) Schematic diagram of the cross-section of the polymer transistor. (b) DPPT-TT polymer transistor optical image. (c) Typical transfer curve and (d) output curve of D-A polymer transistors.

the current. The organic transistors of polymer semiconductors have a low operating frequency of 10 MHz due to their low mobility [27]. Owing to the performance limitations of the oscilloscope used in the experiment, the frequency for this testing method needs to be below 100 kHz to obtain accurate waveform. It should also be noted that the charge pump method needs to consider the effect of geometric components at high frequencies, [28], [29] but the experimental limitations come from the performance of the polymer device under test and the test equipment used. During the gate pulse,

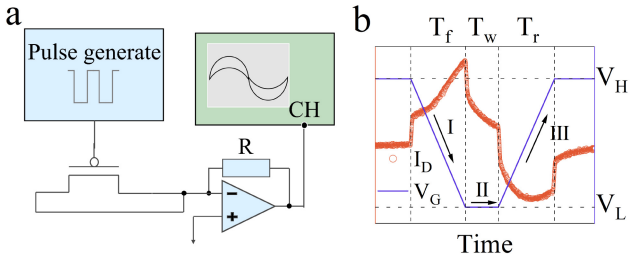

FIGURE 2. **(a) Basic schematic of the device and setup for dynamic pumping. (b) Current waveform and applied gate voltage during measurement.**

the pump current received by the trans-impedance amplifier is converted into a voltage signal and displayed on an oscilloscope. Fig. 2(b) illustrates the results. The gate pulse can be divided into three distinct phases: falling, holding, and rising. During the falling phase, the trap state captures the charge carrier, which is subsequently released during the rising phase. The pulse voltage's fall time, hold time, and rise time is denoted by T_f, T_w, and T_r, respectively. The maximum and minimum pulse voltage values are V_H and V_L.

Equation (1) indicates that the current during the rising and falling phases can be decomposed into two components. A portion of the current, I_d, is driven by the change in concentration of charge carriers caused by the change in gate voltage. As the Fermi energy level rises and falls, the interface trap captures and releases charge carriers, resulting in the second component, the pumping current I_c. The total current is described as:

$$I_{cp} = I_d + I_c \tag{1}$$

By varying the fall time T_f under constant V_H and V_L conditions, Fig. 3(a) illustrates the impact on the peak pumping current. I_{cp}^{max} decreases as T_f increases. Fixed $T_f = T_r = T_w = 50\ \mu s$. As shown in Fig. 3(b), the pumping current rapidly decreases as V_L increases from −40 V to −15 V. Concurrently, the rising phase current becomes gradually flat. This suggests that the minimum interface state exists in the region where V_L=0 V to V_L=−15 V corresponds to the energy level range. In contrast to inorganic semiconductors, where the current decreases quickly during the holding phase, the pumping current decreases gradually [30], [31]. The holding time also influences the pumping current and its integral during the rising phase. Fig. 3(c) exemplifies the pumping current waveforms at various T_w. The increase in pumping current during the rising phase as T_w is increased indicates that the interface states continue to capture charge carriers following the down phase and that there are still interface states that have not yet trapped charge carriers after the falling phase. Extending the holding time consequently increases the number of interface states that capture charge carriers and the number of charge carriers released during the rising phase, resulting in a larger pumping current.

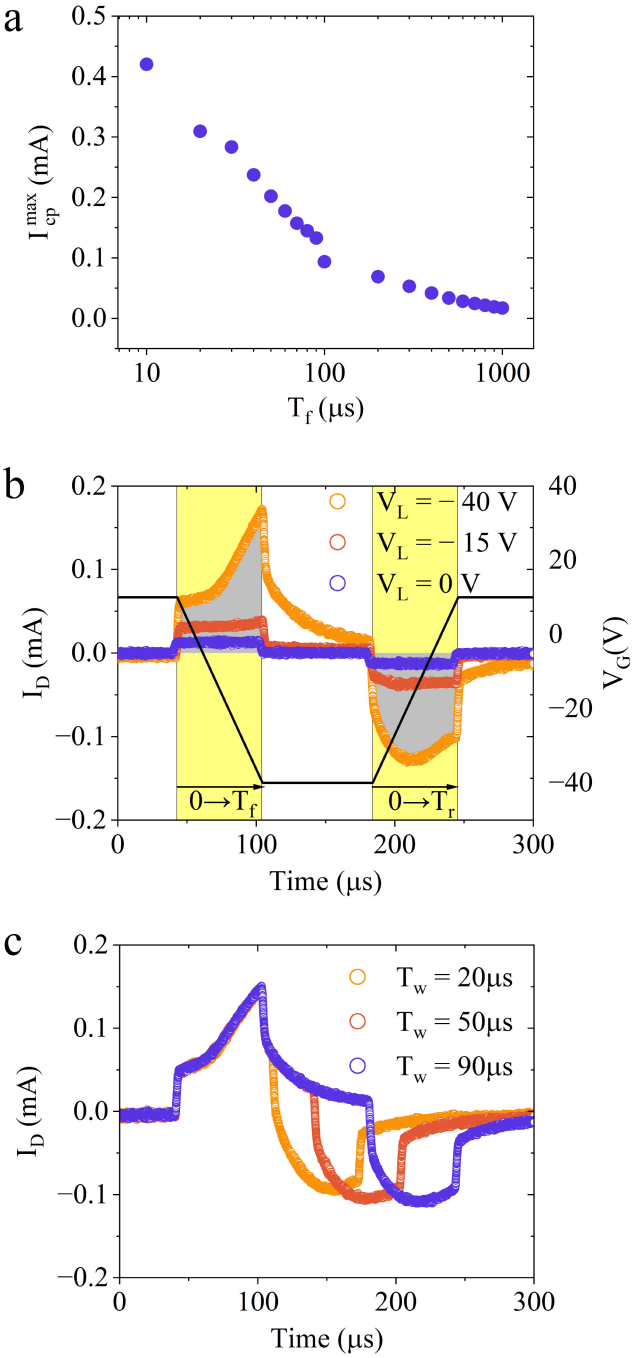

FIGURE 3. **(a) The influence of the fall time on peak pumping current and pumping current under different V_L(b) and T_W(c).**

For a more comprehensive understanding of the dynamic pumping process, Fig. 4 provides a visual representation of how the channel is charged and discharged in the dynamic pumping process. E_i is close to the centre of the bandgap, and the donor-like and acceptor-like states are, respectively, below and above it [32], [33]. Below the Fermi level, the acceptor-like state has a negative charge while the donor-like state has a neutral charge. If the negative charges trapped in the acceptor-like state during the falling phase are not

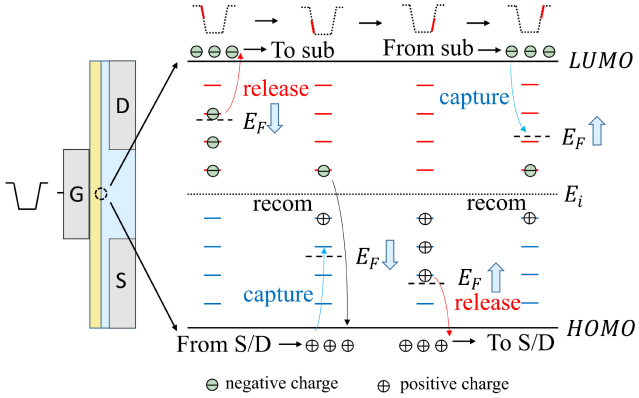

FIGURE 4. Energy band diagrams at different pulse stages.

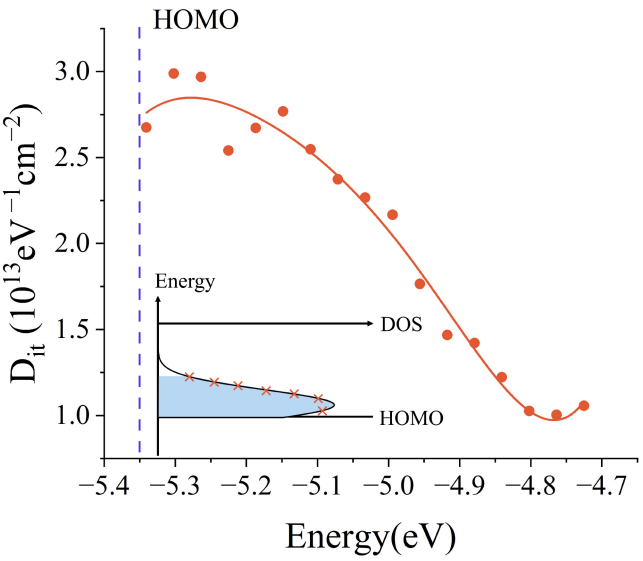

FIGURE 5. State density above HOMO level of DPPT-TT, as extracted by dynamic pumping method.

released to the lowest unoccupied molecular orbital (LUMO) before inversion, they will recombine with the HOMO positive charge carriers following inversion. In addition, charging currents arise when charge carriers are trapped in donor states above the Fermi level. The recombination current and charging current combine to form the peak of the pumping current. During the rising phase, the LUMO negative charges and the donor-like state undergo recombination, while the HOMO negative charges charge the donor-like state.

We extracted the interfacial state distribution above the HOMO level using the dynamic pumping method, as shown in Fig. 5. The interfacial density initially increases and then decreases, reaching a maximum of 3×10^{13} eV^{-1}cm^{-2} with an energy of −5.3 eV. The dynamic pumping method yields greater results than the subthreshold swing method (1.24×10^{12} eV^{-1}cm^{-2}) for calculating the interfacial density of states. This difference is due to the subthreshold swing method's assumption that the density of trap states does not vary with energy. This method can only provide

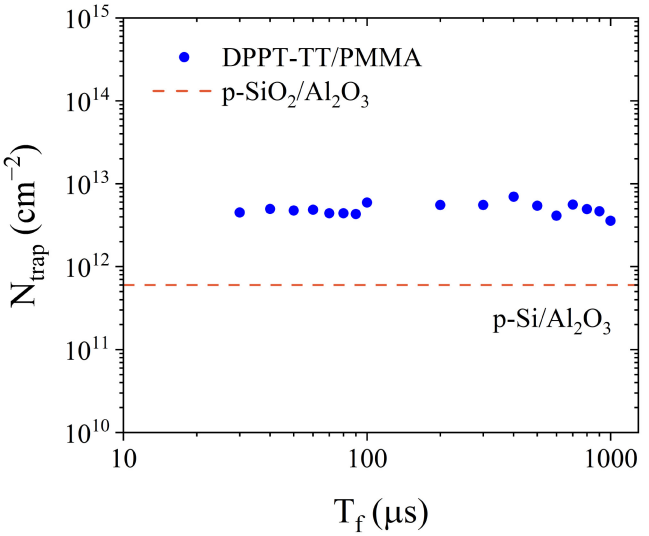

FIGURE 6. Interface states are calculated under different fall times.

an approximate estimate for traps slightly above the Fermi level [34].

Comparing the pumping currents during the rising and falling phases reveals the interface trap density of the transistor. According to (1), the magnitudes of the current I_d during the rise and fall phases are identical, whereas the magnitudes of I_c vary due to the different charge carrier release and trapping times. It is possible to calculate the integral of I_{cp} during the rising and falling phases, and the difference between the charge ΔQ flowing into and out of the source and drain during these two phases is given by (2):

$$\Delta Q = \int_0^{T_f} I_{cp} dt + \int_0^{T_r} I_{cp} dt \tag{2}$$

The interface trap density, denoted by N_{trap}, can be calculated with the help of the following (3). L, and W represent the channel's length and width, while q is the electron's charge constant.

$$N_{trap} = \Delta Q/(qLW) \tag{3}$$

The calculated trap density of the transistor interface at different fall times is presented in Fig. 6. The densities are stable on a temporal scale between 4×10^{12} cm^{-2} and 7×10^{12} cm^{-2}. The results of dynamic pumping indicate that the distribution of polymeric interfacial states in the bandgap may be more concentrated in a particular range than that of inorganic semiconductors. Given that the majority of interfacial states in the corresponding energy range are already involved in the process of dynamic pumping, this may explain why the density of interfacial states does not increase with decreasing time. This phenomenon may be associated with the interfacial energy distribution of polymeric materials.

The trap density and interfacial state distribution for various interfaces are summarized in Table 1. Various techniques, including charge pumping [25], [38], Berglund

TABLE 1. The density and calculation methods of organic and inorganic semiconductor interface states.

Interface	Trap density (cm^{-2})	State density ($eV^{-1}cm^{-2}$)	Years	D_{it} analysis method	Refs.
IGZO/SiO_2	6×10^{10}	$10^9 \sim 10^{14}$	2018	Charge pumping	25
Si/HfO_2	2.8×10^{12}	$10^{11} \sim 10^{13}$	2008	Berglund analysis	35
SiN/AlGaN	-	$10^{10} \sim 10^{14}$	2012	Photo-assisted high frequency CV characterization	36
$Al_2O_3/p-Si$	6×10^{11}	$1\times10^{12} \sim 5 \times 10^{12}$	2019	Conductance	37
$Al_2O_3/In_{0.53}Ga_{0.47}As$	7×10^{10}	$10^{11} \sim 10^{12}$	2008	Charge pumping	38
D139/PDPP-TBT	1.6×10^{11}	$10^{11} \sim 10^{16}$	2012	Kalb and Batlogg	39
Pentancene/SiO_2	-	$10^{10} \sim 10^{13}$	2011	Kelvin probe force microscopy	40
DPPT-TT/PMMA	6×10^{12}	$1\times10^{13} \sim 3.75 \times 10^{13}$	2023	Charge pumping	this work

analysis [35], optically assisted high-frequency CV characterization [36], conductivity [37], and Kelvin probes [40] were utilized to investigate the interfacial states. According to Table 1, the trap density of DPPT-TT/PMMA is 6×10^{12} $eV^{-1}cm^{-2}$, which is greater than that of other organic and inorganic semiconductors. And the interfacial density distribution of DPPT-TT/PMMA is concentrated in the range of $1 \times 10^{13} \sim 3.75 \times 10^{13}$ $eV^{-1}cm^{-2}$.The interface trap density of Al_2O_3/p-Si as determined by the conductometric method is $6 \times 10^{11}cm^{-2}$, and the density of states is stable in the range of $10^{12} \sim 5 \times 10^{12}$ $eV^{-1}cm^{-2}$ [37]. Using the charge pumping technique as well, the IGZO/SiO_2 interface has a trap density of $6 \times 10^{10}cm^{-2}$, while the interface state density spans a wide range from 10^9 to 10^{14} $eV^{-1}cm^{-2}$ [25].

Compared to previous results, the PMMA/DPPT-TT interface states are relatively numerous (Table 1), but they can exhibit higher performance than other previous classes of polymer transistors. This may be caused by the following features: (1) The interaction of the two polymers (PMMA and DPPT-TT) at the interface greatly increases the structural disorder at the interface [41]. (2) The presence of Donor and Acceptor units near the interface exacerbates the energy disorder [42]. However, it should be noted that since these disorders are not like dislocations or vacancies in inorganic systems, their effects consist mainly of carrier transport perturbations and interchain transport disturbances [43]. This also suggests that there is a lot of room for improvement in Donor-Acceptor polymer transistors.

Due to the fact that an OFET is a three-terminal device, it is difficult to measure the substrate current I_{sub}, therefore the influence of the geometric component was not considered in this experiment and will require further investigation in subsequent experiments [28], [29]. The dynamic pumping technique can measure traps located at and near the DPPT-TT/PMMA interface, which periodically capture and release charge carriers under gate voltage pulse control.

In conclusion, the time-domain dynamic pumping of polymeric DPPT-TT field-effect transistors clarifies the charge carrier capture and emission processes. During the falling phase in gate voltage, charge carriers are captured by the interfacial state, resulting in current peaks. The phenomenon of dynamic pumping in polymer transistors differs from that of inorganic semiconductor transistors, which may be a result of the hopping mode of charge carrier transport. Finally, the distribution of the interfacial states of the transistor is analyzed, and it is determined that the density of interfacial states does not vary significantly across time scales.

REFERENCES

[1] X. Wang, Z. Liu, and T. Zhang, "Flexible sensing electronics for wearable/attachable health monitoring," *Small*, vol. 13, no. 25, 2017, Art. no. 1602790. [Online]. Available: https://onlinelibrary.wiley.com/doi/abs/10.1002/smll.201602790

[2] C. Chitrakar, E. Hedrick, L. Adegoke, and M. Ecker, "Flexible and stretchable bioelectronics," *Materials*, vol. 15, no. 5, p. 1664, 2022. [Online]. Available: https://www.mdpi.com/1996-1944/15/5/1664

[3] K. Meng et al., "Wearable pressure sensors for pulse wave monitoring," *Adv. Mater.*, vol. 34, no. 21, 2022, Art. no. 2109357. [Online]. Available: https://onlinelibrary.wiley.com/doi/abs/10.1002/adma.202109357

[4] W. Heng, S. Solomon, and W. Gao, "Flexible electronics and devices as human–machine interfaces for medical robotics," *Adv. Mater.*, vol. 34, no. 16, 2022, Art. no. 2107902. [Online]. Available: https://onlinelibrary.wiley.com/doi/abs/10.1002/adma.202107902

[5] K. Meng et al., "Kirigami-inspired pressure sensors for wearable dynamic cardiovascular monitoring," *Adv. Mater.*, vol. 34, no. 36, 2022, Art. no. 2202478. [Online]. Available: https://onlinelibrary.wiley.com/doi/abs/10.1002/adma.202202478

[6] N. Akhtar et al., "Fabrication of photo-electrochemical biosensors for ultrasensitive screening of mono-bioactive molecules: The effect of geometrical structures and crystal surfaces," *J. Mater. Chem. B*, vol. 5, vol. 39, pp. 7985–7996, 2017. [Online]. Available: http://dx.doi.org/10.1039/C7TB01803G

[7] W. Wang et al., "High-transconductance, highly elastic, durable and recyclable all-polymer electrochemical transistors with 3D micro-engineered interfaces," *Nano-Micro Lett.*, vol. 14, no. 1, p. 184, 2022. [Online]. Available: https://doi.org/10.1007/s40820-022-00930-5

[8] H.-W. Zhu et al., "Printable elastic silver nanowire-based conductor for washable electronic textiles," *Nano Res.*, vol. 13, no. 10, pp. 2879–2884, 2020. [Online]. Available: https://doi.org/10.1007/s12274-020-2947-x

[9] S. Chun, D. W. Kim, J. Kim, and C. Pang, "A transparent, glue-free, skin-attachable graphene pressure sensor with micropillars for skin-elasticity measurement," *Nanotechnology*, vol. 30, no. 33, May 2019, Art. no. 335501. [Online]. Available: https://dx.doi.org/10.1088/1361-6528/ab1d99

[10] M. Estrada et al., "Frequency and voltage dependence of the capacitance of MIS structures fabricated with polymeric materials," *IEEE Trans. Electron Devices*, vol. 60, no. 6, pp. 2057–2063, Jun. 2013. [Online]. Available: https://doi.org/10.1109/TED.2013.2258921

[11] C. S. S. Sangeeth, P. Stadler, S. Schaur, N. S. Sariciftci, and R. Menon, "Interfaces and traps in pentacene field-effect transistor," *J. Appl. Phys.*, vol. 108, no. 11, 2010, Art. no. 113703. [Online]. Available: https://doi.org/10.1063/1.3517085

[12] H. Hirwa, S. Pittner, and V. Wagner, "Interfaces analysis by impedance spectroscopy and transient current spectroscopy on semiconducting polymers based metal–insulator–semiconductor capacitors," *Org. Electron.*, vol. 24, pp. 303–314, Sep. 2015. [Online]. Available: https://www.sciencedirect.com/science/article/pii/S1566119915001925

[13] S. Demirezen and S. A. Yerişkin, "Frequency and voltage-dependent dielectric spectroscopy characterization of Al/(coumarin-PVA)/p-Si structures," *J. Mater. Sci. Mater. Electron.*, vol. 32, no. 20, pp. 25339–25349, 2021. [Online]. Available: https://doi.org/10.1007/s10854-021-06993-1

[14] P. J. Diemer et al., "Quantitative analysis of the density of trap states at the semiconductor-dielectric interface in organic field-effect transistors," *Appl. Phys. Lett.*, vol. 107, no. 10, 2015, Art. no. 103303. [Online]. Available: https://doi.org/10.1063/1.4930310

[15] W. L. Kalb, F. Meier, K. Mattenberger, and B. Batlogg, "Defect healing at room temperature in pentacene thin films and improved transistor performance," *Phys. Rev. B, Condens. Matter*, vol. 76, Nov. 2007, Art. no. 184112. [Online]. Available: https://link.aps.org/doi/10.1103/PhysRevB.76.184112

[16] Y. Yadav and S. P. Singh, "Effect of dielectric surface passivation on organic field-effect transistors: Spectral analysis of the density of trap-states," *Semicond. Sci. Technol.*, vol. 37, no. 1, Dec. 2021, Art. no. 15015. [Online]. Available: https://dx.doi.org/10.1088/1361-6641/ac3c97

[17] S. Singh and Y. Mohapatra, "Bias stress effect in solution-processed organic thin-film transistors: Evidence of field-induced emission from interfacial ions," *Organic Electron.*, vol. 51, pp. 128–136, Dec. 2017. [Online]. Available: https://www.sciencedirect.com/science/article/pii/S1566119917304457

[18] C.-H. Kim, "Bias-stress effects in diF-TES-ADT field-effect transistors," *Solid-State Electron.*, vol. 153, pp. 23–26, Mar. 2019. [Online]. Available: https://www.sciencedirect.com/science/article/pii/S003811011830563X

[19] S. W. M. Hatta et al., "Energy distribution of positive charges in gate dielectric: Probing technique and impacts of different defects," *IEEE Trans. Electron Devices*, vol. 60, no. 5, pp. 1745–1753, May 2013. [Online]. Available: https://doi.org/10.1109/TED.2013.2255129

[20] G. Groeseneken, H. Maes, N. Beltran, and R. De Keersmaecker, "A reliable approach to charge-pumping measurements in MOS transistors," *IEEE Trans. Electron Devices*, vol. 31, no. 1, pp. 42–53, Jan. 1984. [Online]. Available: https://doi.org/10.1109/T-ED.1984.21472

[21] J. Brugler and P. Jespers, "Charge pumping in MOS devices," *IEEE Trans. Electron Devices*, vol. 16, no. 3, pp. 297–302, Mar. 1969. [Online]. Available: https://doi.org/10.1109/T-ED.1969.16744

[22] M. Ekström, B. G. Malm, and C.-M. Zetterling, "Ultrafast pulsed IV and charge pumping interface characterization of low-voltage n-channel SiC MOSFETs," *Mater. Sci. Forum*, vol. 1004, Jul. 2020, pp. 642–651. [Online]. Available: https://doi.org/10.4028/www.scientific.net/MSF.1004.642

[23] A. K. Ghosh, O. O. Awadelkarim, and J. Hao, "Studies of AC BTI stress in 4H SiC MOSFETs," in *Proc. IEEE Int. Integr. Rel. Workshop (IIRW)*, 2021, pp. 1–4. [Online]. Available: https://doi.org/10.1109/IIRW53245.2021.9635608

[24] L. Lin et al., "A single pulse charge pumping technique for fast measurements of interface states," *IEEE Trans. Electron Devices*, vol. 58, no. 5, pp. 1490–1498, May 2011. [Online]. Available: https://doi.org/10.1109/TED.2011.2122263

[25] M.-C. Nguyen et al., "Application of single-pulse charge pumping method on evaluation of indium gallium zinc oxide thin-film transistors," *IEEE Trans. Electron Devices*, vol. 65, no. 9, pp. 3786–3790, Sep. 2018. [Online]. Available: https://doi.org/10.1109/TED.2018.2859224

[26] K. Taniguchi, N. Fang, and K. Nagashio, "Direct observation of electron capture and emission processes by the time domain charge pumping measurement of MoS_2 FET," *Appl. Phys. Lett.*, vol. 113, no. 13, 2018, Art. no. 133505. [Online]. Available: https://doi.org/10.1063/1.5048099

[27] U. Zschieschang, U. Waizmann, J. Weis, J. W. Borchert, and H. Klauk, "Nanoscale flexible organic thin-film transistors," *Sci. Adv.*, vol. 8, no. 13, 2022, Art. no. eabm9845. [Online]. Available: https://www.science.org/doi/abs/10.1126/sciadv.abm9845

[28] L. Lu, M. Wang, and M. Wong, "Geometric effect elimination and reliable trap state density extraction in charge pumping of polysilicon thin-film transistors," *IEEE Electron Device Lett.*, vol. 30, no. 5, pp. 517–519, May 2009. [Online]. Available: https://doi.org/10.1109/LED.2009.2017037

[29] T. Russell, C. Wilson, and M. Gaitan, "Determination of the spatial variation of interface trapped charge using short-channel MOSFET's," *IEEE Trans. Electron Devices*, vol. 30, no. 12, pp. 1662–1671, Dec. 1983. [Online]. Available: https://doi.org/10.1109/T-ED.1983.21428

[30] S. Alghamdi, M. Si, H. Bae, H. Zhou, and P. D. Ye, "Single pulse charge pumping measurements on GaN MOS-HEMTs: Fast and reliable extraction of interface traps density," *IEEE Trans. Electron Devices*, vol. 67, no. 2, pp. 444–448, Feb. 2020. [Online]. Available: https://doi.org/10.1109/TED.2019.2961090

[31] M. Jaiswal and R. Menon, "Polymer electronic materials: A review of charge transport," *Polym. Int.*, vol. 55, no. 12, pp. 1371–1384, 2006. [Online]. Available: https://onlinelibrary.wiley.com/doi/abs/10.1002/pi.2111

[32] J. F. Zhang, S. Taylor, and W. Eccleston, "Electron trap generation in thermally grown SiO_2 under Fowler–Nordheim stress," *J. Appl. Phys.*, vol. 71, no. 2, pp. 725–734, 1992. [Online]. Available: https://doi.org/10.1063/1.351334

[33] G. A. Scoggan and T. P. Ma, "Effects of electron-beam radiation on MOS structures as influenced by the silicon dopant," *J. Appl. Phys.*, vol. 48, no. 1, pp. 294–300, 1977. [Online]. Available: https://doi.org/10.1063/1.323376

[34] W. L. Kalb and B. Batlogg, "Calculating the trap density of states in organic field-effect transistors from experiment: A comparison of different methods," *Phys. Rev. B, Condens. Matter*, vol. 81, Jan. 2010, Art. no. 35327. [Online]. Available: https://link.aps.org/doi/10.1103/PhysRevB.81.035327

[35] P. K. Hurley et al., "Interface defects in HfO_2, $LaSiO_x$, and Gd_2O_3 high-k/metal–gate structures on silicon," *J. Electrochem. Soc.*, vol. 155, no. 2, p. G13, Dec. 2007. [Online]. Available: https://dx.doi.org/10.1149/1.2806172

[36] R. Yeluri, B. L. Swenson, and U. K. Mishra, "Interface states at the SiN/AlGaN interface on GaN heterojunctions for ga and N-polar material," *J. Appl. Phys.*, vol. 111, no. 4, 2012, Art. no. 43718. [Online]. Available: https://doi.org/10.1063/1.3687355

[37] H. Kim and B. J. Choi, "Si surface Passivation by atomic layer deposited Al_2O_3 with in-situ H_2O prepulse treatment," *Trans. Electr. Electron. Mater.*, vol. 20, no. 4, pp. 359–363, 2019. [Online]. Available: https://doi.org/10.1007/s42341-019-00126-6

[38] H. C. Chiu et al., "Achieving a low interfacial density of states in atomic layer deposited Al_2O_3 on $In_{0.53}Ga_{0.47}As$," *Appl. Phys. Lett.*, vol. 93, no. 20, 2008, Art. no. 202903. [Online]. Available: https://doi.org/10.1063/1.3027476

[39] T.-J. Ha, P. Sonar, B. Cobb, and A. Dodabalapur, "Charge transport and density of trap states in balanced high mobility ambipolar organic thin-film transistors," *Org. Electron.*, vol. 13, no. 1, pp. 136–141, 2012. [Online]. Available: https://www.sciencedirect.com/science/article/pii/S1566119911003442

[40] S. Yogev, E. Halpern, R. Matsubara, M. Nakamura, and Y. Rosenwaks, "Direct measurement of density of states in pentacene thin film transistors," *Phys. Rev. B, Condens. Matter*, vol. 84, Oct. 2011, Art. no 165124. [Online]. Available: https://link.aps.org/doi/10.1103/PhysRevB.84.165124

[41] R. Noriega et al., "A general relationship between disorder, aggregation and charge transport in conjugated polymers," *Nat. Mater.*, vol. 12, no. 11, pp. 1038–1044, 2013. [Online]. Available: https://doi.org/10.1038/nmat3722

[42] D. Di Nuzzo et al., "How intermolecular geometrical disorder affects the molecular doping of donor–acceptor copolymers," *Nat. Commun.*, vol. 6, no. 1, p. 6460, 2015. [Online]. Available: https://doi.org/10.1038/ncomms7460

[43] H. Sirringhaus, M. Bird, and N. Zhao, "Charge transport physics of conjugated polymer field-effect transistors," *Adv. Mater.*, vol. 22, no. 34, pp. 3893–3898, 2010. [Online]. Available: https://onlinelibrary.wiley.com/doi/abs/10.1002/adma.200902857